Engineering Structures 260 (2022) 114253

Contents lists available at ScienceDirect

Engineering Structures

journal homepage: www.elsevier.com/locate/engstruct

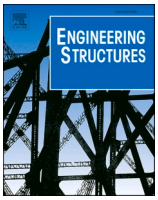

Active isolation tests of metamaterial-based barriers and foundation

Jiaji Wang [a,*], Hsuan Wen Huang [b], Benchen Zhang [c], F.-Y. Menq [d], Kalyana Babu Nakshatrala [e], Y.L. Mo [f], K.H. Stokoe [g]

[a] Postdoctoral associate, Corresponding author, University of Houston, Houston, Texas, USA
[b] University of Houston, Houston, Texas, USA
[c] The University of Texas at Austin, Austin, Texas, USA
[d] Operations Manager, The University of Texas at Austin, Austin, Texas, USA
[e] Associate Professor, University of Houston, Houston, Texas, USA
[f] John and Rebecca Moores Professor, University of Houston, Houston, Texas, USA
[g] Jennie C. and Milton T. Graves Chair Professor, The University of Texas at Austin, Austin, Texas, USA

ARTICLE INFO

Keywords:
Active isolation test
Shaker
Exciting frequency
Excitation direction
Periodic barrier
Periodic foundation

ABSTRACT

This study investigates the performance of novel metamaterial-based barriers and foundation on mitigating waves transmitting from a vibrational source to the surrounding soil. An active isolation system is a wave barrier built close to the vibration source to reduce the wave radiating from the source of vibration on the structure to surrounding soil. This research reports the efficacy of the proposed isolation system using an active excitation field test, thereby expanding the applicability of such wave barriers beyond passive isolation. The test barrier is a trench barrier infilled with a layered periodic metamaterial that is composed of alternating layers of polyurethane and reinforced concrete (RC). Tests are also conducted on an empty trench for comparison. A mobile shaker mounted on top of a steel frame is utilized to simulate an active vibration source. By mechanically reorienting the shaker, active isolation tests can be conducted in all three directions (vertical, horizontal inline, and horizontal crossline). Motions on the ground surface, periodic barrier, foundation, and steel frame are monitored using three-dimensional (3D) geophones and 3D accelerometers. The effects of the barrier length, the infilled material, and the total number of barriers on the isolation behavior at various exciting frequencies, and excitation directions are investigated. Tests also include the scenario where the wave barrier is used along with a metamaterial-based periodic foundation. Experimental studies show that vibrations generated from the shaker mounted on top of the steel frame are effectively restrained by a metamaterial-based foundation. The performance of the periodic barriers is better than that of an empty trench within certain frequency ranges. The wave isolation performance is enhanced with the increasing barrier length. This research provides the benchmark for the future design of periodic barriers and periodic foundations in buildings or other vibration-sensitive facilities.

1. Introduction

Earthquakes have always posed a great threat to lives, infrastructure, and the economy. The damage will be devastating when structural systems are poorly designed or constructed. A significant number of damages in structural systems during seismic events have been reported. To prevent seismic damage to the structures, different seismic isolation systems were reported and tested in the literature. Isolation of the structure from ground vibrations by wave barriers installation was widely studied experimentally, numerically and adopted in engineering practice. The vibrations in soil may include notable body wave and surface wave content. Since the energy of the surface wave decays more slowly than the body wave, the wave barrier is generally built close to the ground surface to prevent the surface wave from transmitting into the protected region. Based on the installation location, the wave barriers may be categorized as either passive isolation or active isolation barriers [1-5]. When the source of the vibrations is known, to contain the vibration within a certain region, the barrier that is installed near the vibration source is an active isolation barrier. When the barrier is installed close to the protected region to provide destructive

* Corresponding author.
E-mail addresses: jj-wang14@tsinghua.org.cn, jwang215@central.uh.edu (J. Wang), hhuang15@uh.edu (H.W. Huang), thebens@utexas.edu (B. Zhang), fymenq@utexas.edu (F.-Y. Menq), knakshatrala@uh.edu (K.B. Nakshatrala), yilungmo@central.uh.edu (Y.L. Mo), k.stokoe@mail.utexas.edu (K.H. Stokoe).

https://doi.org/10.1016/j.engstruct.2022.114253
Received 4 August 2021; Received in revised form 15 March 2022; Accepted 5 April 2022
Available online 15 April 2022

interference of wave entering the protected region, the wave barrier is classified as a passive isolation barrier [6]. For example, preventing earthquake ground motion from entering a certain structure is a passive isolation topic, while preventing the vibration to trabsfer from heavy machines in industrial buildings to surrounding soil and surrounding structures is an active isolation problem [7]. In addition, preventing the traffic-induced vibration from railway bridges to transfer to surrounding structures is also active isolation problem. The active isolation periodic barrier is investigated in this research.

Empty trenches and infilled trenches are two typical forms of wave barriers [6,8-23]. Woods [6] reported a full-scale experimental study in the free field to investigated the active and passive wave mitigation performance of the empty trench barrier. Several numerical and experimental studies were reported and met some degree of success in isolating the vibration. Finite element (FE) [10,15,18-20,23,24] and boundary element methods (BEM) [9,16] are widely used by researchers to understand the behavior of wave barriers. Due to the complexity of soil, the simplified numerical model may not be sufficient to always represent the true behavior observed on the test site. Recently, more and more lab experiments [14,25] and field tests [10-13,18] were conducted for the sake of understanding the real performance of the wave barrier in the soil. Investigations on the effect of the infilled material, geometry, and the barriers numbers on the wave isolation of the wave barrier were widely studied. However, the effect of the exciting frequency [11,12,18] and the excitation direction were rarely the focus of the earlier research.

The periodic material can also be referred to as metamaterial [26], which is a composite material arranged periodically and possess special property to mitigate the harmonic wave within its frequency band gap, which is a material property and can be optimized to cover very wide frequency ranges. The governing equation of wave propagation is scalable, and the dimension of the metamaterial is proportional to the magnitude of wavelengths corresponding to the frequency band gap [27]. Since most structures generate energy in the lower frequency range, the corresponding wavelengths are relatively large [28]. As a result, the length scale of the periodic material applied to manipulate the seismic wave is larger compared to noise isolation or heat isolation metamaterials. The periodic foundation is the base isolation system that is made of the periodic metamaterial [29-38]. This innovative seismic isolation system changes the pattern of the earthquake energy when the internal structure of the periodic foundation interacts with the incoming waves. The experimental results showed that the periodic foundations can mitigate both horizontal and vertical seismic waves in their frequency band gap, thereby reducing the resulting response on the superstructure. Researchers [39-43] carried out several studies regarding the 1D or 2D periodic material for earthquake isolation. With a shake table, the excitation can be uniformly applied directly to the bottom of the periodic foundation. The shake table experiment on the 1D periodic foundation was reported by Xiang et al. [44]. The 1D periodic foundation is made of layers of rubber and concrete. The results had shown a significant response reduction within the specific frequency ranges. From the shake table test, a 50% reduction of peak horizontal response and a 15.9% reduction of peak vertical response were observed when the exciting frequency fell into the frequency band gaps. Large-scale 1D and 3D periodic foundations with superstructure scaled from a real small modular reactor were built [36,37]. The tests prove that the periodic foundation is capable of filtering the waves having frequencies inside its frequency band gap for vertical, horizontal, and torsional modes. By comparing the peak acceleration responses for cases with and without the periodic foundation, a 90% reduction was observed. The superstructure was isolated by the periodic foundation without introducing large relative displacement. Field experiments of scaled 2D and 3D periodic foundations were conducted [31,32] to validate the finite element simulation. The unit cell of the periodic foundation is made of iron, rubber, and reinforced concrete. The iron core coated with polyurethane is covered by the reinforced concrete at the outer layer. Using the shakers, Rattler and Thumper, at the University of Texas at Austin, the excitations were applied on the ground surface in the vertical and horizontal directions. By comparing the response on the steel frame for cases with and without the periodic foundation, the periodic foundation is proved to be effective to filter out the S wave and P wave with the exciting frequencies within its frequency band gap [45].

1D Periodic barriers or 1D metamaterial-based barriers are infilled barriers composed of 1D layered periodic material [45-49]. The periodic material used in this study is composed of the unit cell with polyurethane layers and concrete layers alternatively. The periodic barrier, which embeds the periodic material in the soil and is not directly attached to the structure, is expected to work as a non-invasive isolation measure for the existing structure. Being a non-invasive seismic isolation system, the periodic barrier does not need to support a heavy superstructure and is easier for maintenance. Therefore, the periodic barriers will be of tremendous value to the earthquake engineering community worldwide. A large-scale periodic barrier called seismic metamaterial, in the form of periodically arranged boreholes with the depth of 5 m, was fabricated and studied [50]. The seismic wave was generated by a monochromatic vibrocompaction probe. This large-scale experiment showed the feasibility of seismic metamaterial in modifying the seismic energy distribution for civil engineering applications. The screening effectiveness was shown that the signal hardly passed the second row of boreholes. However, the higher energy intensity was detected in the area near the source after the boreholes were carried out. The combination of the periodic barrier and periodic foundation is expected to result in total isolation for the underground structure. Huang et al. [48] and Zhang et al. [51] investigated the passive isolation performance of combined usage of periodic barrier and periodic foundation using state-of-the-art T-Rex shaker. Based on field test results, the combined performance of periodic barrier and periodic foundation achieved broadband wave isolation performance from 15 Hz to 100 Hz in vertical excitation and horizontal excitation.

In this study, the periodic barriers and empty trenches are investigated in field tests. Other than the infilled material, the other parameters of the wave barrier are emphasized, including the barrier length, the number of barriers, the exciting frequency, and the excitation directions. A hydraulic shaker, Thumper, is placed on top of the steel frame to generate excitation to the structure in the active isolation test. The RC foundation and periodic foundation are presented in the first and second scenarios respectively. The reduction of soil particle velocity due to the adoption of metamaterial-based barrier installation is presented. The efficiency of the periodic barrier, periodic foundation, and the combined usage of periodic barrier and periodic foundation for active isolation tests is reported in detail. Section 2 reports the test matrix, loading facility, specimen design, and measurement details of the field test for the active isolation test. Section 3 describes the result interpretation to quantify the performance of the barriers. Section 4 presents the experimental results including the reduction of ground surface response and filtering capability of the periodic barrier and periodic foundation.

2. Experimental setup

Fig. 1 shows the nomenclature and test matrix in this study. Two scenarios of active isolation tests are conducted. The first scenario of tests with the RC foundation is denoted as A1; the second scenario of tests with the periodic foundation is denoted as A2. In each scenario, there are four different barrier conditions as well as a benchmark case without a barrier. As shown in Fig. 1, these four barrier conditions are investigated: (1) EL (empty long trench); (2) B1: a single short metamaterial-based barrier; (3) B2: two identical short metamaterial-based barriers (denoted as B2); (3) BL: a single long metamaterial-based barrier. The benchmark case refers to the condition without the presence of the barrier and is denoted as S0. The empty trench (denoted as EL) and the long barrier (denoted as BL) share the same dimension, which has the depth, length, and thickness of 1.52 m, 2.44 m, and 0.28 m, respectively. The cases B1 and B2 have the depth, length, and

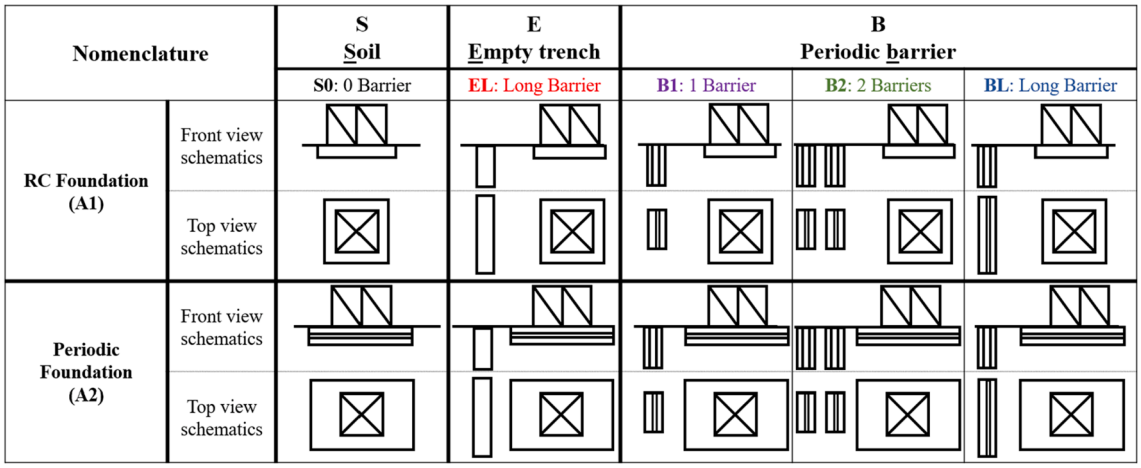

Fig. 1. Nomenclature and test setup schematics.

thickness of 1.52 m, 1.22 m, and 0.28 m, respectively. The periodic barrier is a sandwiched specimen with a single polyurethane layer (0.08 m thick) and two layers of RC slab (each slab has a thickness of 0.1 m). A single layer of No. 4 reinforcing bars (13 mm diameter) is applied in the RC slab with a spacing of 130 mm in both directions. The yield strength of reinforcement is 413.7 MPa based on the rebar coupon test. The size of the metamaterial-based foundation is 1.37 m × 0.91 m × 0.51 m. The size of the RC foundation is 0.76 m × 0.76 m × 0.13 m. The periodic foundation is manufactured using three layers of 101.6 mm (4 in.) thick RC slabs, and two layers of polyurethane, with the bottom layer of polyurethane being 127 mm in thickness and the top layer being 76.2 mm in thickness. The size of the frame structure is 0.6 m × 0.6 m × 0.6 m, which is connected using slotted steel angle members (brand name is Everbilt, angle section has equal length of 38 mm and thickness of 2 mm). The section is applied with Zinc coating and is a cold-rolled slotted steel section. The steel frame is connected using bolts. The additional weights of 18.6 kg were connected on the bottom side and top side of the steel frame. The top weight serves as a roof to place the actuator.

The ground surface response is collected by 3D geophones deployed on the ground. Fig. 2 shows the layout of the sensors for the detection of soil response in the test program. The geophone sensors are applied in three directions (including horizontal crossline, horizontal inline, and vertical) as shown in Fig. 2. The structure response is collected by the 3D accelerometers mounted on the steel frame and foundation. The description for the sensor layout, loading protocol, and these four barrier conditions can be found in earlier research [48,51].

Active isolation is defined by the employment of a wave barrier near the vibration source to prevent the wave from leaving the source. To simulate the scenario that the vibration is generated by the machine, a hydraulic mobile shaker (Thumper from NEHRI@UTexas) is placed on the roof of the steel frame. Fig. 3 shows the orientation of the shaker (Thumper) installed on top of the steel frame. By changing the orientation of the shaker, the excitation direction can be controlled in three directions. Three forms of excitations include the seismic waves, the sweep-frequency tests and the fix-frequency harmonic excitation, and the earthquake excitation. The sweep-frequency tests cover the frequency range from 15 Hz to 100 Hz in a total time of 12 s. A total of 9 scaled earthquake seismograms are also selected to include the Chi-Chi earthquake (TCU052), Anza, San Fernando, Gilroy, El Centro, Northridge Oroville, Loma Prieta, Bishop. The performance of the barriers and the periodic foundation are evaluated by the soil and structure response in the same way as what was done for passive isolation tests [45,48].

The tests are conducted at the test site which is a part of the Hornsby Bend Biosolids Management Plant southeast of Austin, Texas. The site investigation was reported in earlier research [45,48] and the soil parameters obtained from spectral analysis of surface waves (SASW) are summarized as follows. The first layer has a depth between 0 and 0.61 m; the second layer has a depth between 0.6 and 2.1 m below the ground surface, and anything beneath the second layer is considered as the third layer. The shear wave velocity is 91.44 m/sec, 161.5 m/sec, and 234.7 m/sec in the first, second, and third layers, respectively. The density measurement suggests at 0.3 m (1 ft) below the ground surface has a density of 1670 kg/m^3, and the density at 0.91 m (3 ft) below the ground surface is 1702 kg/m^3. With the Poisson ratio for the unsaturated soil assumed to be 0.33, the resulting Young's modulus is 20 MPa, 118 MPa, and 249 MPa in the first, second, and third layers, respectively. The theoretical result of frequency band gaps for the periodic barrier and periodic foundation are reported in earlier research [45,48] as listed in Table 1, which was derived using Bloch theory as illustrated by Witarto [33].

3. Evaluation of the barrier performance

The frequency response function (FRF) is a typical measure to

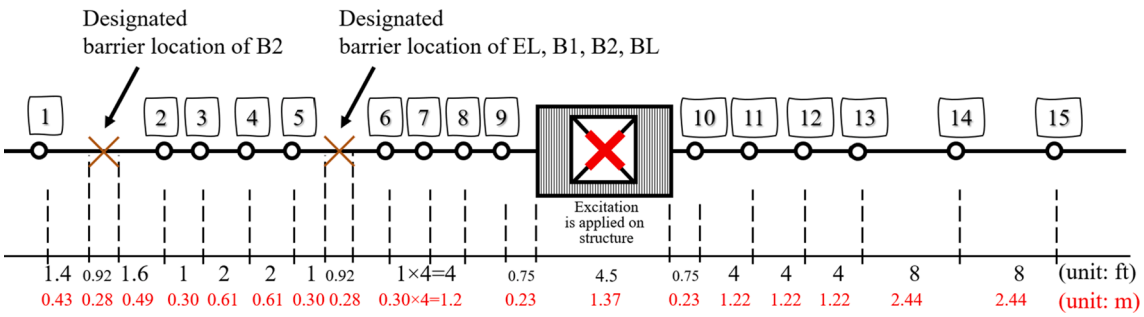

Fig. 2. Geophone deployment in active isolation tests.

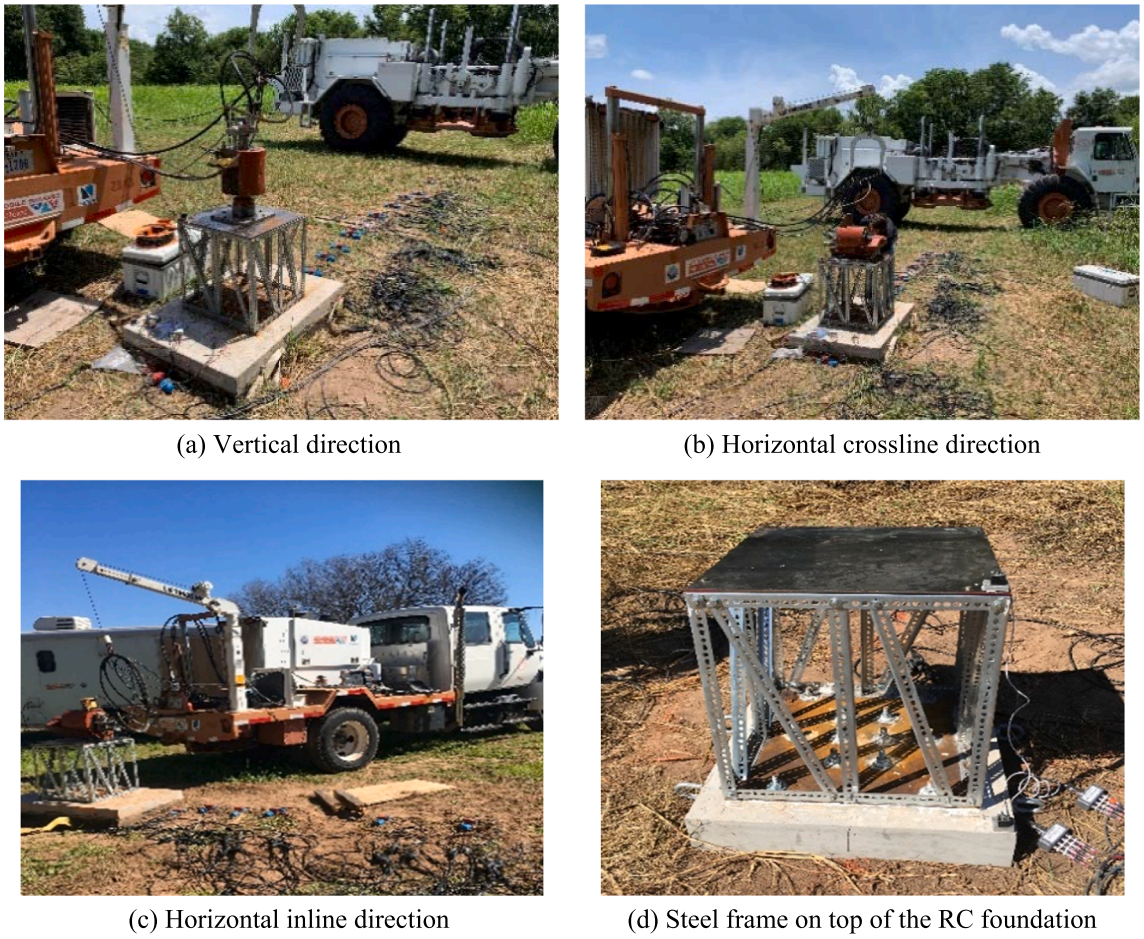

(a) Vertical direction (b) Horizontal crossline direction

(c) Horizontal inline direction (d) Steel frame on top of the RC foundation

Fig. 3. Orientation of the shaker (Thumper) installed on top of the steel frame.

Table 1
Theoretical frequency band gaps of metamaterial-based barrier and metamaterial-based foundation [45,48]

Specimen	Wave type	Theoretical frequency band gaps
Periodic barrier	P wave (longitudinal wave)	45.0–100 Hz
	S (shear wave)	11.8–46.1, 49.1–92.1, and 93.7–100 Hz
	Rayleigh wave	10.2–43.8, 47.0–87.6, and 88.8–100 Hz.
Periodic foundation	P wave (longitudinal wave)	32–39.7 and 54.9–100 Hz
	S (shear wave)	8.4–10.4, 14.4–48.5, and 49.2–100 Hz.

quantify the screening effectiveness of periodic material, including both barriers and foundations. Two different approaches are adopted for calculating FRF, the "Average method" and "Direct method" in Eq. (1) and Eq. (2) respectively. Similar approaches were also reported in detail by Huang et al. [45,48]. The average method takes the response at all sensors within a certain area into account while the direct method divides the acceleration at the two critical measurement locations adjacent to the barrier or foundation to calculate FRF.

$$\overline{FRF}(f) = \frac{1}{5}\sum_{i=1}^{5}[20\log_{10}(\frac{A(f)_{exit,i}}{A(f)_{enter}})] \quad (1)$$

$$FRF(f) = 20\log_{10}\left(\frac{A(f)_{exit}}{A(f)_{enter}}\right) \quad (2)$$

where $A(f)_{exit,i}$ is the response at the ith measurement point at the exiting side of the wave barriers. For average method, the *FRF* is obtained by taking an average over an extent from Point No. 1 to Point No. 5 (measuring extent equal to 2.44 m as shown in Fig. 2).$A(f)_{exit}$ is the response at the exiting face of the periodic material, and $A(f)_{exit}$ is the response at the entering face of the periodic material. The entering face and the exiting face are at the first and the last layer of the periodic material, either the periodic barrier or periodic foundation. The FRF of the periodic foundation is only evaluated using the direct method. The response is first converted to the frequency domain for the calculation. For earthquake excitation, after obtaining the FRF for each earthquake event, the averaged FRF results from a total of 9 seismic wave tests are reported.

4. Experimental results

4.1. Soil particle response in fix-frequency harmonic tests

To compare the response between different barrier conditions in fixed-frequency tests, the following steps are used to define the normalized acceleration of soil particles measured at points No. 1–9 shown in Fig. 2: (1) Numerical difference was adopted to convert the original triaxial velocity signal of Geophone sensors to acceleration sensors; (2) the total velocity magnitude is calculated based on velocity components in three directions; (3) fast Fourier transformation is used to convert the total velocity data from time domain to frequency domain; (4) the acceleration at soil particle is normalized by the force output (in units of N) from the Thumper shaker. The force output of Thumper shaker is obtained by multiplying the acceleration at the moving mass of

Thumper shaker by its mass (193 kg) as reported by Menq et al. [52]. Fig. 4 shows the comparison of normalized response at certain excitation frequencies in each excitation direction.

The geometric decay for each barrier condition is observed for all cases, indicating a notable damping effect of soil for all cases. In the vertical excitation test, Fig. 4 (a) shows that the soil particle acceleration of the benchmark case (A1S0) is higher than all barrier conditions. The response of case A1BL is found to be similar to the case A1EL, which shows that the wave isolation behavior of the periodic barrier reaches that of the empty trench that has the same dimension. Under vertical excitation, the Rayleigh wave is the dominant wave type transmitting in soil and barrier. As shown in Table 1, 15 Hz is within the theoretical frequency band gap of periodic barriers. Therefore, Case A1BL shows notable wave mitigation performance as shown in Fig. 4(a).

In the horizontal crossline excitation test, Fig. 4(b) shows that the soil particle acceleration of the benchmark case (A1S0) is higher than all barrier conditions. Case A1B1 and Case A1EL achieve best wave mitigation performance in the region under horizontal crossline excitation. Under horizontal crossline excitation, S wave the dominant wave type transmitting in soil and barrier. As shown in Table 1, 15 Hz is within the theoretical frequency band gap of periodic barriers for shear wave. Therefore, Case A1B1 shows notable wave mitigation performance as shown in Fig. 4(a).

In the horizontal inline excitation test at excitation frequency of 15 Hz, Fig. 4(c) shows that Case A1B2 achieves the most notable wave mitigation performance and Case A1B1 shows slightly higher response compared to Case A1S0, A1EL and A1BL. At excitation frequency of 50 Hz, Fig. 4(d) shows that empty trench (A1EL) achieves best wave isolation performance while A1BL also notably reduce the soil particle velocity. P wave is the dominant wave component transferring in soil and barrier under horizontal inline excitation. As shown in Table 1, the P wave with excitation frequency of 15 Hz is in the pass band of the periodic barrier while 50 Hz is in band gap periodic barrier. Therefore, the test results of periodic barrier shown in Fig. 4(d) is notably better than that of Fig. 4(c).

In addition, the results in Fig. 4 shows that the soil particle response may vary at different measuring points. Therefore, the average method is adopted in Section 4.2 to evaluate the wave isolation performance of barriers with global information. In comparison, the Direct method in Section 4.3 evaluates the wave isolation performance of barriers with localized information by directly comparing both the response on both surfaces of barrier.

4.2. *FRF of barriers obtained from the average method*

This section presents the *FRF* results obtained from the Average method for each barrier condition and excitation. The *FRF* is obtained by taking an average over an extent from Point No. 1 to Point No. 5 (measuring extent equal to 2.44 m as shown in Fig. 2). When the *FRF* obtained from the Average method is below 0, the attenuation zones are identified. Fig. 5 shows the FRF results obtained by the Average method in the earthquake excitation for all test scenarios. In Fig. 5, the excitation direction and measurement sensor direction are the same and the theoretical frequency band gaps are marked in yellow color in each plot. In this study, the theoretical frequency band gap marked in yellow color in Fig. 5 was only used to design the periodic barrier and periodic foundation. Because the wave component in soil particle in active isolation field tests are very complicated, it is very hard to generate a specific wave type in this test program. For example, in horizontal inline excitation, the structure foundation may be subject to a combination of

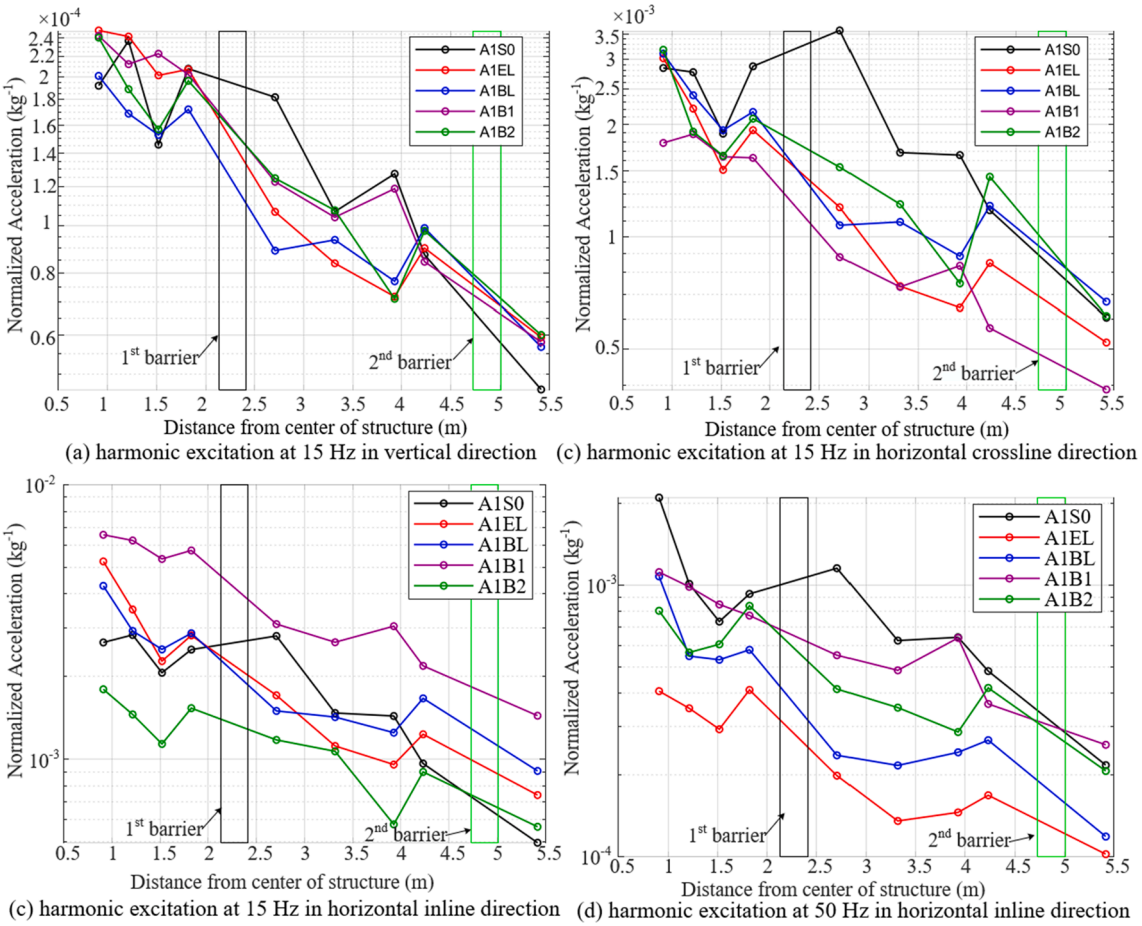

Fig. 4. Fix-frequency test results of normalized acceleration of soil particles.

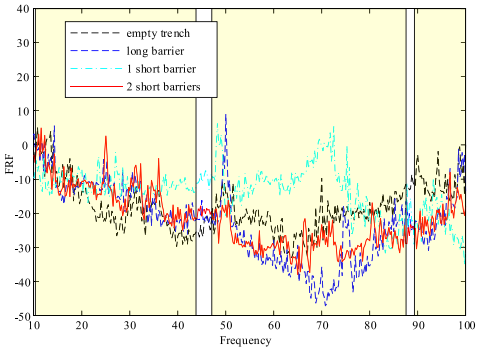

(a) Vertical exictation FRF compared to frequency band gap of Rayleigh wave

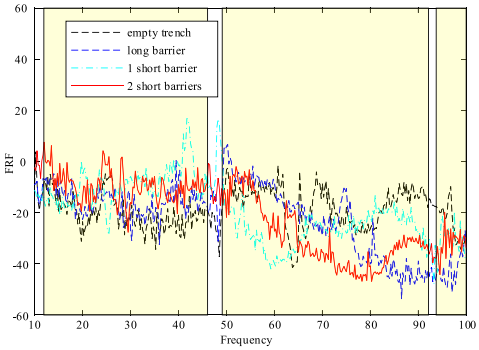

(b) Horizontal crossline excitation FRF compared to freuqnecy band gap of S wave

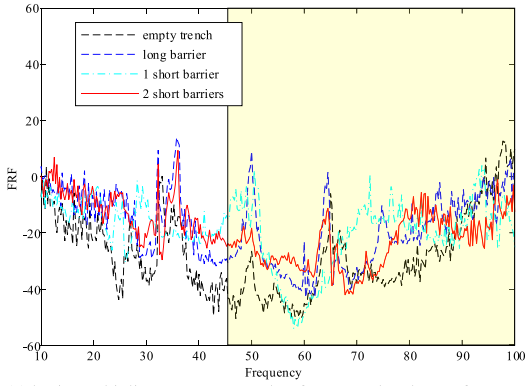

(c) horizontal inline FRF compared to frequency band gap of P wave

Fig. 5. *FRF* obtained from soil particle acceleration using the average method and seismic tests of A1 case with concrete foundation Note: the excitation direction and measurement sensor direction are the same. The theoretical frequency band gaps are marked in yellow color in each plot.

horizontal shear force and overturning moment, which may generate a combination of Rayleigh wave and P wave in soil particle. Therefore, FRF results from field test may not fit exactly to theoretical frequency band gap. Future research will be focused on developing high-fidelity finite element model of the test program with model updating algorithm to achieve best fit with test results.

As shown in Fig. 5(a), under vertical excitation, one short barrier showed relatively less wave isolation performance. This may be attributed to the fact that the length of short barrier was half of long barrier, and may not mitigate the wave transferred outside its length. Long barrier (A1BL) achieved best wave isolation performance for frequency higher than 50 Hz, while empty trench (A1EL) showed most notable wave mitigation performance for excitation frequency below 50 Hz. In the theoretical frequency band gap of Rayleigh wave, 2 short barriers (A1B2) and long barrier (A1BL) both show notable wave isolation performance, which is consistent with the theoretical result.

As shown in Fig. 5(b), under horizontal crossline excitation, one short barrier (A1B1) showed amplified response at the theoretical pass band of S wave (i.e., 46.1 to 49.1 Hz). Long barrier (A1BL) and 2 short barriers (A1B2) both showed better wave isolation performance compared to empty trench (A1EL) for frequency higher than 50 Hz, while various wave barriers had similar performance for excitation frequency below 50 Hz. In theoretical band gap of S wave, long barrier (A1BL) and 2 short barriers (A1B2) both showed notable wave isolation performance.

As shown in Fig. 5(c), under horizontal inline excitation, empty trench showed best wave isolation performance in frequency range from 10 Hz to 88 Hz. In frequency band gap of P wave, two short barriers (A1B2) show notable wave isolation mitigation performance. Metamaterial-based barriers mostly showed wave isolation performance for the theoretical frequency band gap of P wave.

The effect of the barrier length can be seen by comparing A1BL and A1B1 because these two barrier conditions have the same infilled material, which is the 1D layered periodic material. Because the influenced zone shielded by the barrier is larger when the barrier is longer, the performance of the long barrier is generally better than that of short barrier.

4.3. *FRF of barriers obtained from the direct method*

To exclude the soil layer's contribution in evaluating the FRF of barriers, the Direct method uses the response at two critical sensor locations to calculate the *FRF*. These two critical locations are selected to be at the sensor locations in the front and the back of the barrier and these two sensor locations are denoted as Point No. 6A and Point No. 5A respectively in Fig. 6. To capture the response at these two locations, two accelerometers are added at the two edges of the one short periodic barrier (B1).

The response at these two sensor locations, Point No.5A and Point No. 6A, is collected by the accelerometer at the edges of the first and the last layer of the periodic barrier. Fig. 7 shows the barrier response at these two critical sensor locations when one short periodic barrier is presented and frequency sweeping excitation is applied on top of the steel frame in scenario A1B1, where the steel frame is installed on top of a traditional concrete foundation. As shown in Fig. 7, a significant reduction of acceleration is observed in the frequency and time domain in all three directions tested. Therefore, the performance of the periodic barrier is verified using the acceleration measurement results of Fig. 7.

The other set of the active isolation tests that involve the periodic foundation is denoted as the A2B1 scenario. Fig. 8 shows the response at these two critical sensor locations as the periodic foundation is used to hold the steel frame and the shaker. The effectiveness of the periodic barrier observed in the A2B1 scenario in Fig. 8 is still observed. However, the effectiveness is not as notable as the A1B1 scenario as shown in Fig. 7. The reason is summarized as follows: the periodic foundation filters the wave, so the response at the entering face of the periodic barrier is much smaller than the A1B1 scenario. The wave is afterward filtered again by the periodic barrier, but since the signal is significantly smaller already, the reduction of acceleration is less notable in the A2B1 scenario. In addition, based on comparison of results in Fig. 7 and Fig. 8, material nonlinearity and damping in elastic response may notably contribute to the performance of periodic barrier. The material nonlinearity and damping are recommended to be considered in future finite element simulation of periodic barriers based on Fig. 7 and Fig. 8.

Fig. 9 shows the *FRF* calculated by the Direct method for all test cases from seismic tests. The theoretical frequency band gaps are highlighted in the yellow patches. The direct method results in Fig. 9 is similar to that of Fig. 5 obtained from average method. As shown in Fig. 9(a), under vertical excitation, 2 short barriers showed most notable wave isolation performance. In the theoretical frequency band gap of Rayleigh wave, metamaterial-based barriers (A1BL, A1B1 and A1B2) all show notable wave isolation performance, which is consistent with the theoretical result. As shown in Fig. 9(b), under horizontal crossline excitation, one short barrier (A1B1) showed amplified response at the theoretical pass band of S wave (i.e., 46.1 to 49.1 Hz). Two short barriers

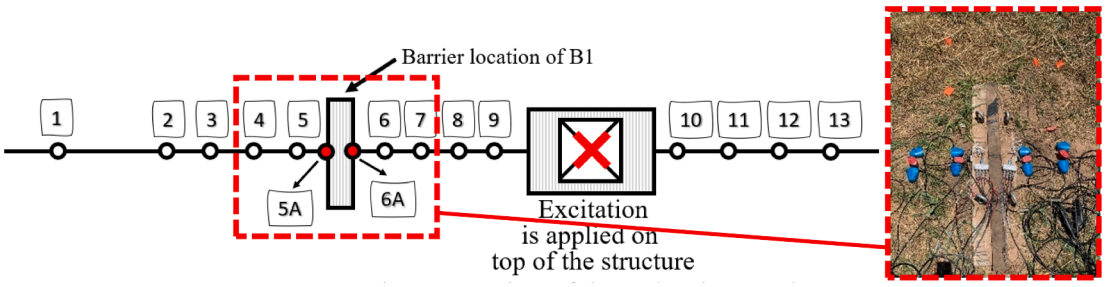

Fig. 6. Top view of the updated sensor layout.

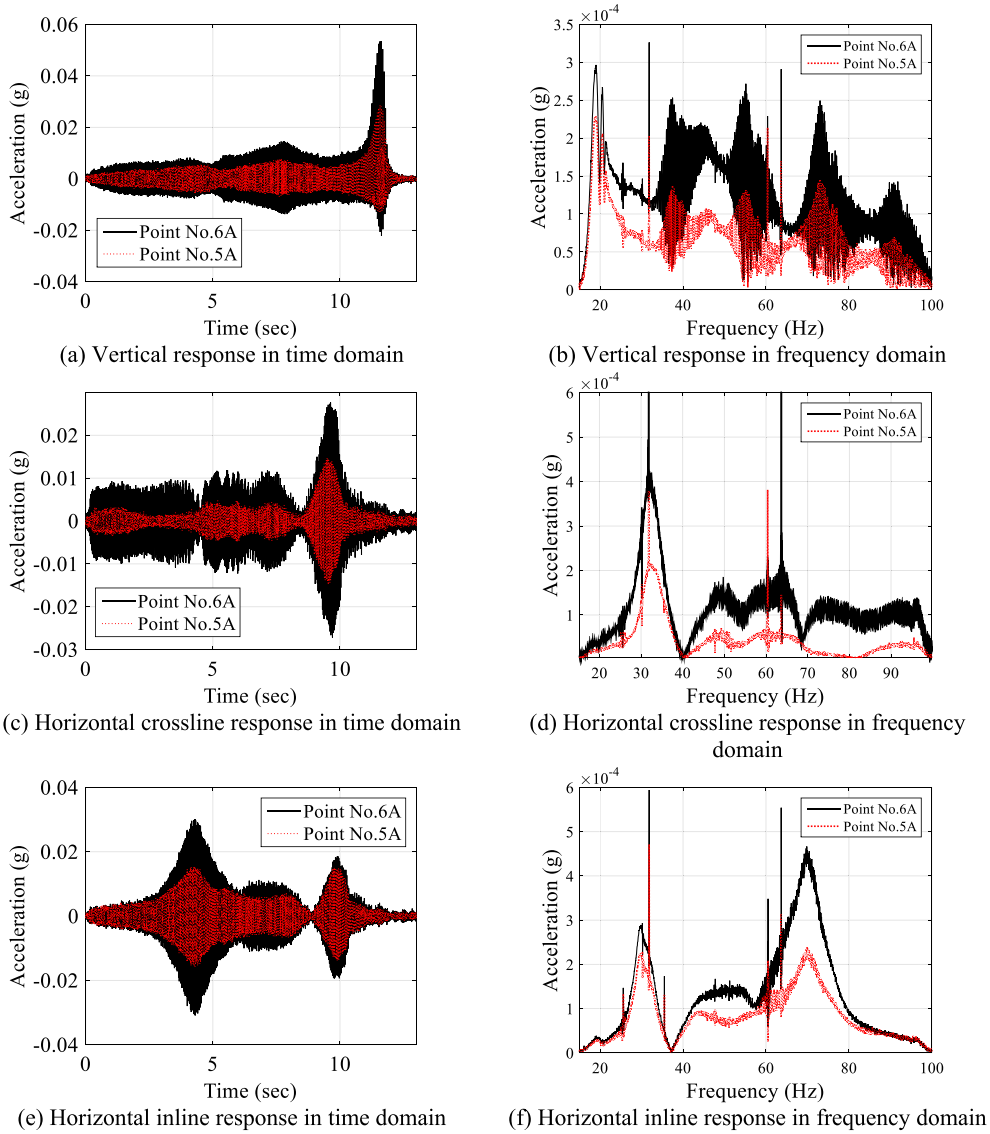

Fig. 7. The response at both sides of periodic barrier in A1B1 scenario at point No. 5A and point No. 6A.

(A1B2) showed better wave isolation performance compared to empty trench (A1EL) for frequency higher than 50 Hz. In theoretical band gap of S wave, long barrier (A1BL) and 2 short barriers (A1B2) both showed notable wave isolation performance. As shown in Fig. 9(c), under horizontal inline excitation, two short barriers (A1B2) show notable wave isolation mitigation performance in frequency band gap of P wave. In general, Fig. 9 shows response reduction within the theoretical band gaps marked in yellow, which is derived from Bloch theory as illustrated by Witarto [33]. Attenuation zones are identified in the majority of frequency range from 15 Hz to 100 Hz for metamaterial-based barriers. Based on the comparison between test results and Bloch theory in Fig. 9, the Bloch wave analysis results failed to predict experimental results. The reason for the discrepancy between Bloch theory and test results may be attributed to the following two reasons: (1) The Bloch wave analysis refers only to infinite periodic media, in the test program, however, the length, depth and number of metamaterial-based barriers are limited in the test. (2) The damping of soil, concrete and rubber material was neglected in Bloch theory, which may also reduce the

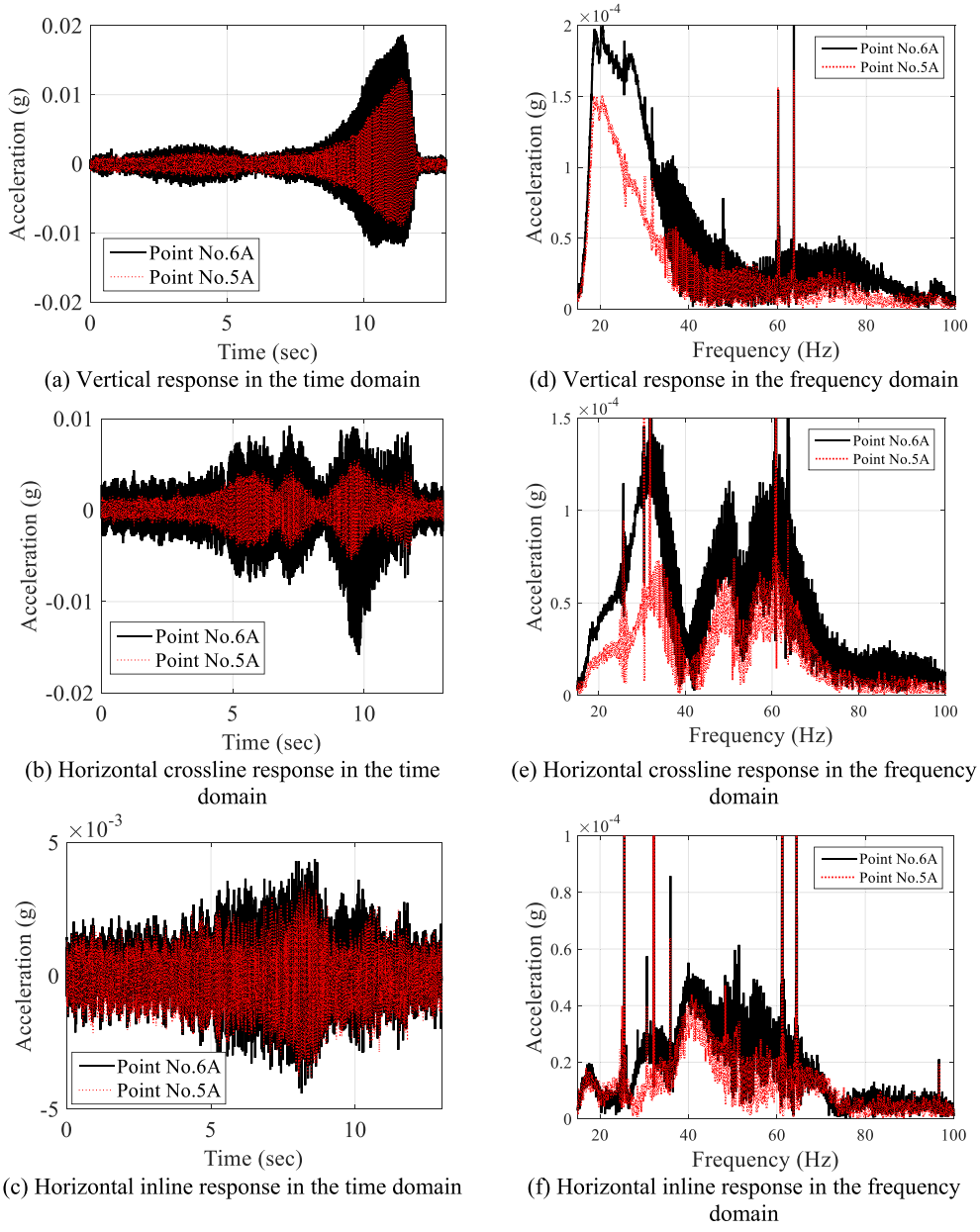

(a) Vertical response in the time domain
(d) Vertical response in the frequency domain
(b) Horizontal crossline response in the time domain
(e) Horizontal crossline response in the frequency domain
(c) Horizontal inline response in the time domain
(f) Horizontal inline response in the frequency domain

Fig. 8. The response at both sides of periodic barrier in A2B1 scenario at 5A and 6A.

response after the wave pass through the metamaterial-based barriers. Therefore, a more elaborate 3D finite element simulation or machine learning approach are recommended for simulating the complicated test program reported in this study.

4.4. *FRF of periodic foundation obtained from direct method*

By placing the 3D accelerometers in the path of wave transmission at the bottom and top of the metamaterial-based foundation, the filtering characteristic of the metamaterial-based foundation can be observed by comparing the response on the bottom and top surface recorded during the same loading event. Therefore, the responses can be directly compared without the need for normalization. Fig. 10 presents the *FRF* results of case A2S0 subjected to excitation in all three directions.

Each sub-plot in Fig. 10 contains the results obtained from the excitation in all three forms (Fix-frequency harmonic, frequency sweeping, and earthquake). It is found that the different forms of input signals display the results agreeing with each other. The attenuation zone is identified as the *FRF* is below zero in Fig. 10. A similar observation found in Section 4.2 is that using a different form of input signal indicates the same attenuation zones for each excitation direction. Their resulting attenuation zones coincide with theoretical band gaps. Under vertical excitations, the dominated wave is assumed to be the P wave, and the theoretical band gaps of metamaterial-based foundation under the P wave are 32–39.7 Hz and 54.9–100 Hz. The amplification in Fig. 10(a) occurs within 46–48 Hz under vertical excitation which is outside its frequency band gap for the P wave. Under horizontal crossline or horizontal inline excitation, the dominated wave is assumed to be the S wave, and the theoretical band gaps of the S wave are 8.4–10.4 Hz, 14.4–48.5 Hz, and 49.2–100 Hz, which was also observed in test results from Fig. 10 (b) and (c).

As reported by Huang [45], the FRF was obtained by the data collected by two sensors on both sides of the metamaterial-based foundation in the passive isolation test (denoted as the P2S0 scenario). In the passive isolation test, the wave is assumed to transfer upward in the periodic foundation. Therefore, the entering face and the exiting face in

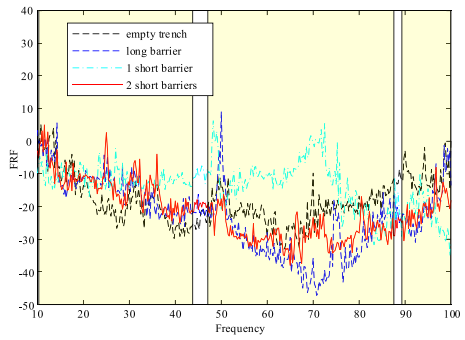

(a) Vertical *FRF* compared to the frequency band gap of Rayleigh wave

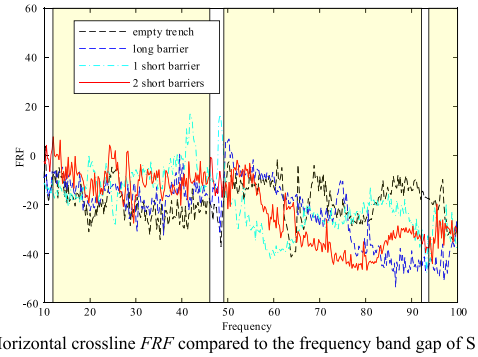

(b) Horizontal crossline *FRF* compared to the frequency band gap of S wave

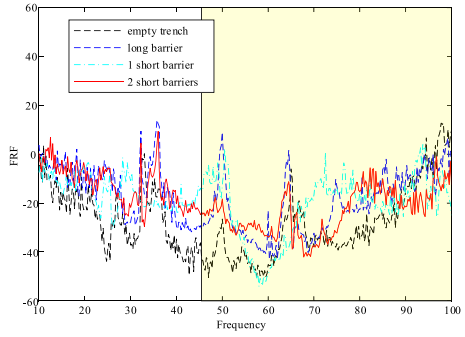

(c) Horizontal inline *FRF* response compared to the theoretical band gap of the P wave

Fig. 9. *FRF* obtained from soil particle acceleration using the direct method and seismic tests Note: the excitation direction and measurement sensor direction are the same. The theoretical frequency band gaps are marked in yellow color in each plot.

Eq. (2) are at the bottom and the top of the periodic foundation respectively for passive isolation tests. Fig. 11 shows the *FRF* of response at the periodic foundation in the benchmark case (P2S0).

By comparing the FRF of the metamaterial-based foundation response between passive isolation tests in Fig. 11 and active isolation tests in Fig. 10, it is found that the attenuation zones identified from active isolation tests match better with the theoretical results than from the passive isolation tests. It is because the wave propagation path is clearer during the active isolation test, so it is easier to determine the dominant wave transmitting through the periodic foundation. When the shaker is generating vertical vibration, the dominating wave through the periodic foundation is the P wave. Under horizontal vibration excitation, the dominant wave is the S wave. The theoretical band gaps of the metamaterial foundations for the P wave and S wave are highlighted. The theoretical band gaps are not exactly the same as the test results of FRF because only one unit cell is adopted in the test program. In addition, the damping of material was not considered in the theoretical analysis, which may also induce the discrepancy between the test and Bloch theory results. In order to achieve better understanding of the test results, the elaborate finite element simulation is recommended.

4.5. *FRF of barrier-foundation system obtained from direct method*

In this section, the combined performance of barrier-foundation system is investigated using Direct method and seismic test results. Fig. 12 shows the comparison of FRF of barrier-foundation system and the FRF of barrier obtained from A2EL case, A2BL case and A2B2 case. To evaluate the FRF of barrier-foundation system, the exit point in Eq. (2) is selected at point No. 5 for A2EL and A2BL or point No. 1 for A2B2 case. The enter point in Eq. (2) is selected at the acceleration at top surface of periodic foundation. As shown in Fig. 12, notable wave isolation performance was observed for barrier-foundation system for all cases (A2EL, A2BL and A2B2) and all three directions. Therefore, by adopting combined usage of metamaterial-based foundation with metamaterial-based barrier, notable vibration isolation can be achieved and the vibration isolation performance is similar to that of empty trench (A2EL). In addition, the FRF of barrier obtained from the same test is also plotted. As shown in Fig. 12, the wave isolation performance of barrier-foundation system is notably improved compared to the FRF of barrier for most frequency range. This is attributed to the fact that the frequency band gaps of metamaterial-based barrier and metamaterial-based foundation are not consistent as illustrated in Table 1 in Section 2. Therefore, by combined usage of metamaterial-based barrier and foundation, a broadband wave isolation result can be achieved from 10 Hz to 100 Hz in all three directions.

4.6. *Effect of reflection induced by the periodic foundation on structure response*

The reflection of vibration from the periodic foundation to the superstructure may induce an unfavorable influence on structural safety under active excitation. The shaker, Thumper, is mounted on top of the steel frame, and the shaker output of acceleration is expected to be the same as the acceleration on the roof of the steel frame. However, a discrepancy exists between these two recorded values. This section intends to see if the reflection from the periodic foundation adversely affects the structure response. The shaker's motion and the resulting response on top of the steel frame of the scenario with the RC foundation (A1S0) and with periodic foundation (A2S0) are shown in Fig. 13.

Fig. 13 (a), (c), and (e) are the results of Case A1S0 with the concrete foundation, and Fig. 13 (b), (d), and (f) are the results of Case A2S0 with the metamaterial-based foundation. The metamaterial-based foundation may reflect the vibration to the structure when the frequency of the excitation falls in its band gaps. When the periodic foundation is used, the response on top of the steel frame is reduced under vertical excitation, while it is amplified under horizontal excitation. In general, adopting a metamaterial-based foundation will not notably enhance the vibration of the structure system when excitation is applied on the higher levels of the structure.

5. Conclusions

In active isolation tests, the barriers are used to contain the vibration to protect the surrounding structures. This paper reports the active isolation test scenario that the vibration is generated by the shaker mounted on top of a steel frame, and the performance of the barrier is assessed by the ground surface response that is shielded behind the barrier. In addition, the barrier response is used to observe the frequency-selective properties of the periodic barrier. Several conclusions can be made from this study.

1. With the test setup that can precisely generate the vibration and record the response in all three directions, the performance is found to be dependent on the direction and frequency of excitation. The barrier length plays an important role in determining the performance of the barrier. The longer barrier showed better wave isolation performance compared to a short barrier.

2. The contribution of the metamaterial-based barrier can be seen by

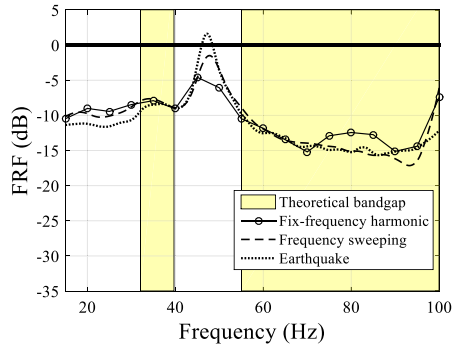

(a) Vertical *FRF* compared to the theoretical band gap of the P wave

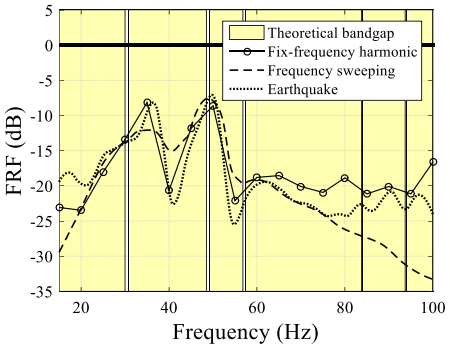

(b) Horizontal crossline FRF compared to the theoretical band gap of S wave

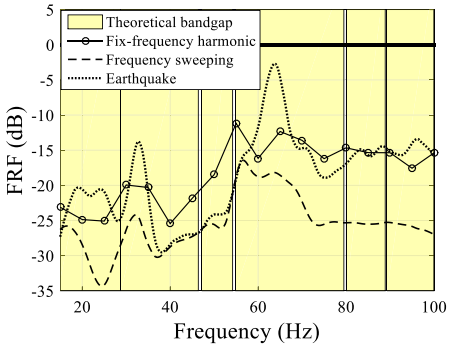

(c) Horizontal inline FRF compared to the theoretical band gap of S wave

Fig. 10. *FRF* of response at the periodic foundation in the benchmark case (A2S0).

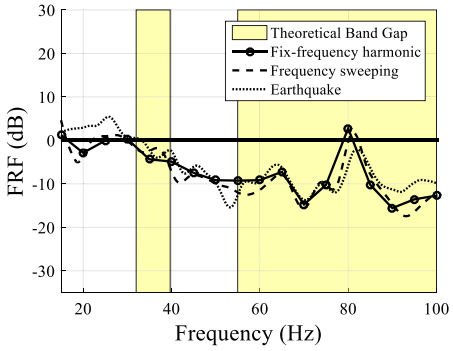

(a) Vertical FRF compared to theoretical frequency band gap of P wave

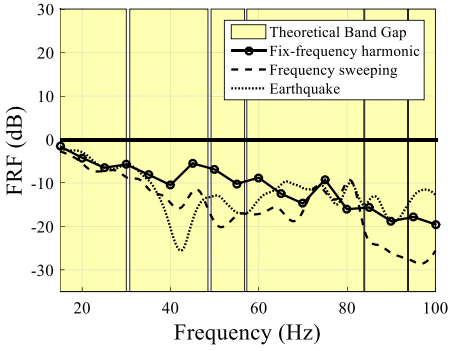

(b) Horizontal crossline FRF compared to theoretical frequency band gap of S wave

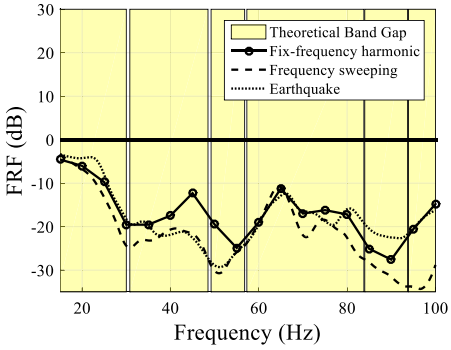

(c) Horizontal inline FRF compared to theoretical frequency band gap of S wave

Fig. 11. *FRF* of response at the periodic foundation in the benchmark case (P2S0) [45]

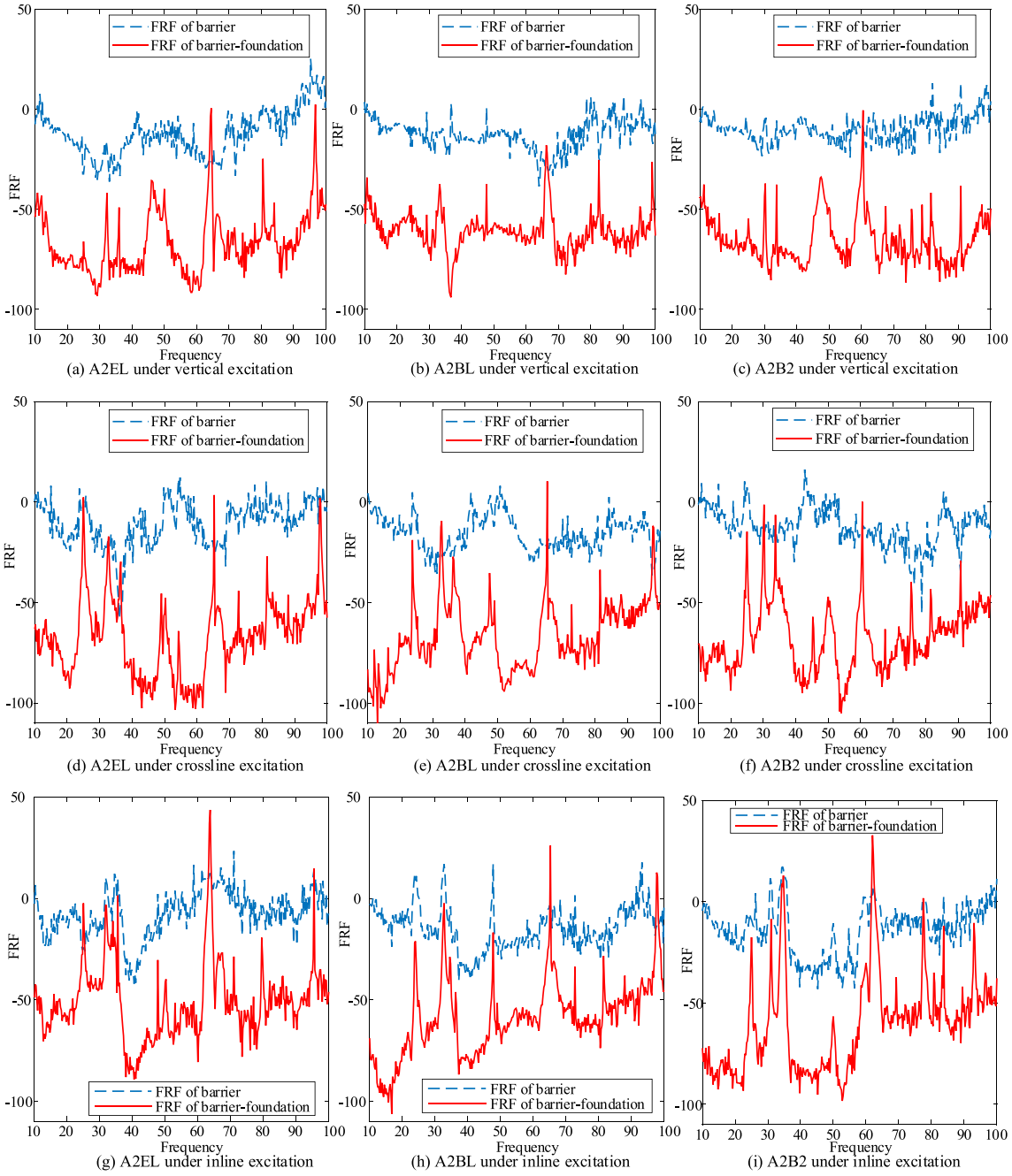

Fig. 12. Frequency response function of barrier-foundation system from seismic excitation.

comparison the performance of one long empty trench and one long periodic barrier. Based on the field test results, A1BL (long barrier) outperforms A1EL (empty trench) within certain frequency ranges under vertical excitation or horizontal crossline excitation.

3. The Average method adopts averaged response at 5 geophone sensors, while Direct method uses the response at the two edges of the periodic barrier to calculate the FRF. The results from Average method and Direct method are consistent. The test FRF of periodic barriers did not agree with theoretical band gaps of the periodic barrier.

4. The filtering capability of the periodic foundation is calculated by the Direct method. The results from three different forms of excitations (fixed-frequency harmonic, frequency sweeping, and earthquake excitation) are found to be highly consistent. The attenuation zones did not agree with the theoretical band gap of metamaterial-based foundation.

5. The FRF of barrier-foundation system is investigated by Direct method by comparing the soil particle acceleration after barrier to the acceleration on top surface of periodic foundation. By combined usage of metamaterial-based barrier and foundation, a broadband wave isolation result can be achieved from 10 Hz to 100 Hz in all three directions.

6. The filtering capability of the periodic foundation raises a concern about the effect of the reflection caused by the periodic foundation on the superstructure. By comparing the shaker output and the motion on the roof of the superstructure when the RC foundation is used and when the periodic foundation is used, the effect of the reflection on the superstructure can be observed. It is found when the periodic foundation is used, the response on top of the steel frame is reduced in vertical loads but amplified in horizontal loading tests.

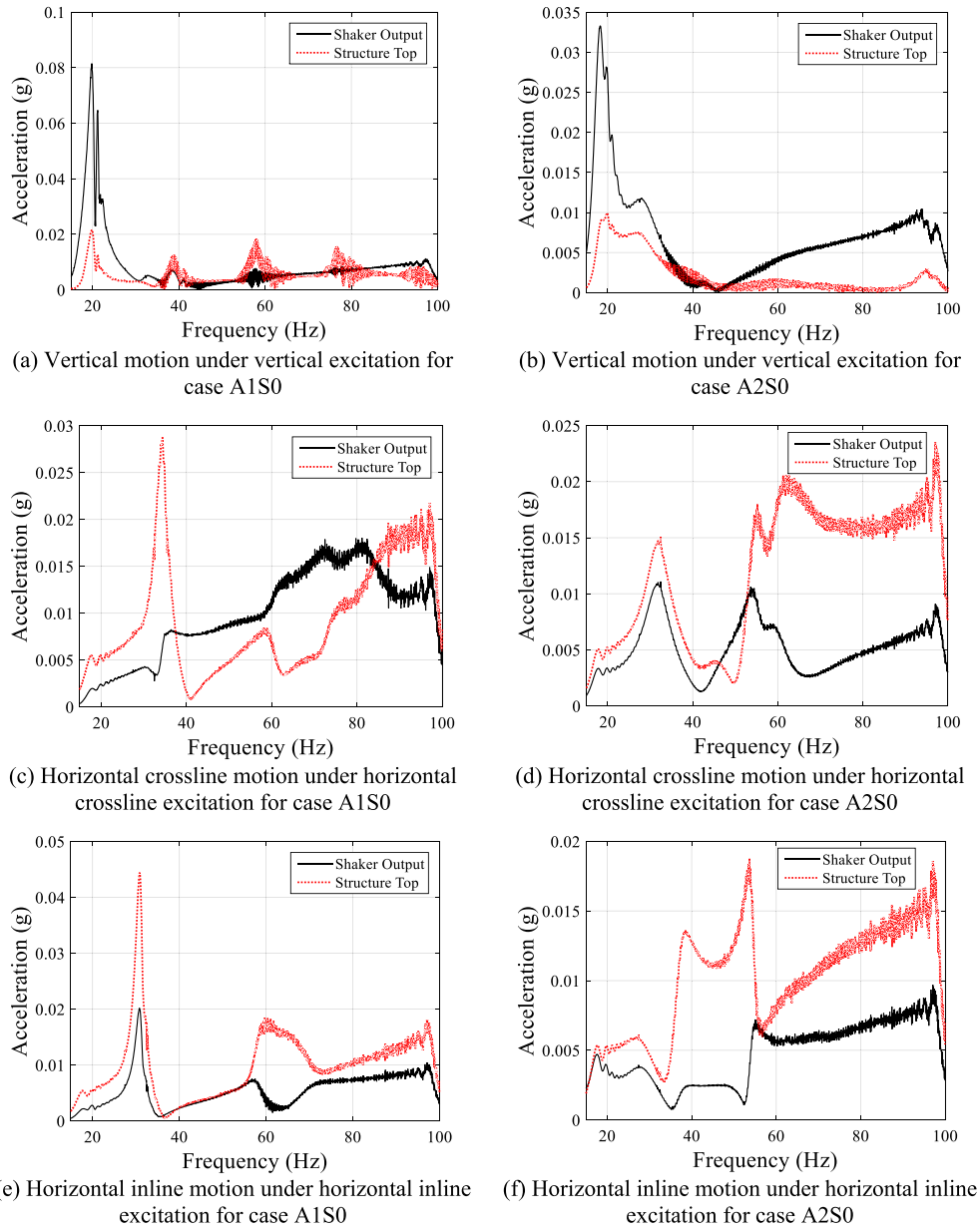

(a) Vertical motion under vertical excitation for case A1S0

(b) Vertical motion under vertical excitation for case A2S0

(c) Horizontal crossline motion under horizontal crossline excitation for case A1S0

(d) Horizontal crossline motion under horizontal crossline excitation for case A2S0

(e) Horizontal inline motion under horizontal inline excitation for case A1S0

(f) Horizontal inline motion under horizontal inline excitation for case A2S0

Fig. 13. Shaker's acceleration and structure response under frequency sweeping excitation.

CRediT authorship contribution statement

Jiaji Wang: Writing – original draft, Writing – review & editing, Methodology, Formal analysis, Visualization. **Hsuan Wen Huang:** Writing – original draft, Writing – review & editing, Methodology, Visualization. **Benchen Zhang:** Investigation, Validation, Data curation. **F. -Y. Menq:** Writing – review & editing, Data curation, Resources. **Kalyana Babu Nakshatrala:** Writing – review & editing, Validation, Supervision. **Y.L. Mo:** Writing – review & editing, Resources, Supervision, Project administration, Funding acquisition. **K.H. Stokoe:** Resources, Supervision, Project administration, Funding acquisition.

Declaration of Competing Interest

The authors declare that they have no known competing financial interests or personal relationships that could have appeared to influence the work reported in this paper.

Acknowledgments

This study is financially supported by the National Science Foundation under grant 1761659. The authors would like to express gratitude to NHERI@UTexas for the experiment execution.

References

[1] Gao G, Li N, Gu X. Field experiment and numerical study on active vibration isolation by horizontal blocks in layered ground under vertical loading. Soil Dyn Earthquake Eng 2015;69:251–61.
[2] Wang JG, Sun W, Anand S. Numerical investigation on active isolation of ground shock by soft porous layers. J Sound Vib 2009;321:492–509.
[3] Richart F, Hail J, Woods R. Vibrations of soils and foundations: prentice-hall. Inc 1970.
[4] Gao GY, Li ZY, Qiu C, Yue ZQ. Three-dimensional analysis of rows of piles as passive barriers for ground vibration isolation. Soil Dyn Earthquake Eng 2006;26:1015–27.
[5] Liao S, Sangrey D. Use of piles as isolation barriers. J Geotech Geoenviron Eng 1978;104:1139–52.
[6] Woods RD. Screening of suface waves in soils: Industry Program of the Colledge of Engineering. The University of Michigan; 1968.

[7] Ding RTMX, Zhou M, Nie JG. Seismic behavior of RC structures with absence of floor slab constraints and large mass turbine as a non-conventional TMD: a case study. Bull Earthquake Eng. 2015;13:3401–22.
[8] AI-Hussaini TM, Ahmad S. Simple design methods for vibration isolation by wave barriers. International Conferences on Recent Advances in Geotechnical Earthquake Engineering and Soil Dynamics 1991.
[9] Al-Hussaini TM, Ahmad S. Design of wave barriers for reduction of horizontal ground vibration. J Geotech Eng 1991;117:616–36.
[10] Alzawi A, El Naggar MH. Full scale experimental study on vibration scattering using open and in-filled (GeoFoam) wave barriers. Soil Dyn Earthquake Eng 2011; 31:306–17.
[11] Andersen L, Nielsen SR. Reduction of ground vibration by means of barriers or soil improvement along a railway track. Soil Dyn Earthquake Eng 2005;25:701–16.
[12] Çelebi E, Fırat S, Beyhan G, Çankaya İ, Vural İ, Kırtel O. Field experiments on wave propagation and vibration isolation by using wave barriers. Soil Dyn Earthquake Eng 2009;29:824–33.
[13] Coulier P, Cuéllar V, Degrande G, Lombaert G. Experimental and numerical evaluation of the effectiveness of a stiff wave barrier in the soil. Soil Dyn Earthquake Eng 2015;77:238–53.
[14] Coulier P, Hunt HE. Experimental study of a stiff wave barrier in gelatine. Soil Dyn Earthquake Eng 2014;66:459–63.
[15] Ekanayake SD, Liyanapathirana D, Leo CJ. Attenuation of ground vibrations using in-filled wave barriers. Soil Dyn Earthquake Eng 2014;67:290–300.
[16] Leung K, Beskos D, Vardoulakis I. Vibration isolation using open or filled trenches. Comput Mech 1990;7:137–48.
[17] Massarsch K. Man-made vibrations and solutions. International Conference on Case Histories in Geotechnical Engineering. 1993.
[18] Persson P, Persson K, Sandberg G. Numerical study of reduction in ground vibrations by using barriers. Eng Struct 2016;115:18–27.
[19] Qiu B. Numerical study on vibration isolation by wave barrier and protection of existing tunnel under explosions: Laboratory of Civil & Environmental Engineering. Inst Nat Sci Appl Lyon 2014.
[20] Segol G, Abel JF, Lee PC. Amplitude reduction of surface waves by trenches. J Eng Mech Div 1978;104:621–41.
[21] Thompson D, Jiang J, Toward M, Hussein M, Ntotsios E, Dijckmans A, et al. Reducing railway-induced ground-borne vibration by using open trenches and soft-filled barriers. Soil Dyn Earthquake Eng 2016;88:45–59.
[22] Ulgen D, Toygar O. Screening effectiveness of open and in-filled wave barriers: a full-scale experimental study. Constr Build Mater 2015;86:12–20.
[23] Waas G. Linear two-dimensional analysis of soil dynamics problems in semi-infinite layer media. Department of Civil and Environmental Engineering. University of California; 1972.
[24] Saikia A. Numerical study on screening of surface waves using a pair of softer backfilled trenches. Soil Dyn Earthquake Eng 2014;65:206–13.
[25] Leilei X. Influence of in-filled trench as wave barrier on ground vibrations. Stockholm: Royal Institute of Technology; 2012. MSc Thesis.
[26] Kittel C. Introduction to Solid State Physics. Hoboken: John Wiley & Sons; 2005.
[27] Kushwaha MS, Halevi P, Dobrzynski L, Djafari-Rouhani B. Acoustic band structure of periodic elastic composites. Phys Rev Lett 1993;71:2022.
[28] Maldovan M. Sound and heat revolutions in phononics. Nature 2013;503:209–17.
[29] Xiang HJ, Shi ZF, Wang SJ, Mo YL. Periodic materials-based vibration attenuation in layered foundations: experimental validation. Smart Mater Struct 2012;21:1–10.
[30] Yan Y, Mo YL, Menq FY, Stokoe II KH, Perkins J, Tang Y. Development of seismic isolation systems using periodic materials. Technical Report Project No. 3219: Department of Energy; 2014.
[31] Yan Y, Laskar A, Cheng Z, Menq F, Tang Y, Mo YL, et al. Seismic isolation of two dimensional periodic foundations. J Appl Phys 2014;116:044908.
[32] Yan Y, Cheng Z, Menq F, Mo YL, Tang Y, Shi Z. Three dimensional periodic foundations for base seismic isolation. Smart Mater Struct 2015;24:075006.
[33] Witarto W. Periodic Material-Based Seismic Base Isolators For Small Modular Reactors. Texas: University of Houston; 2018.
[34] Witarto W, Nakshatrala KB, Mo Y-L. Global sensitivity analysis of frequency band gaps in one-dimensional phononic crystals. Mech Mater 2019;134:38–53.
[35] Witarto W, Wang S, Nie X, Mo Y, Shi Z, Tang Y, et al. Analysis and design of one dimensional periodic foundations for seismic base isolation of structures. Int J Eng Res Appl 2016;6:5–15.
[36] Witarto W, Wang S, Yang C, Nie X, Mo Y, Chang K, et al. Seismic isolation of small modular reactors using metamaterials. AIP Adv 2018;8:045307.
[37] Witarto W, Wang S, Yang C, Wang J, Mo Y, Chang K, et al. Three-dimensional periodic materials as seismic base isolator for nuclear infrastructure. AIP Adv 2019; 9:045014.
[38] Yan Y, Mo Y-L, Menq F-Y, Stokoe I, Kenneth H, Perkins J, et al. Development of seismic isolation systems using periodic materials. LLC, Idaho Falls, ID (United States): Battelle Energy Alliance; 2014.
[39] Jia G, Shi Z. A new seismic isolation system and its feasibility study. Earthquake Eng Eng Vibrat 2010;9:75–82.
[40] Bao J, Shi Z, Xiang H. Dynamic responses of a structure with periodic foundations. J Eng Mech 2012;138.
[41] Cheng Z, Shi Z. Novel composite periodic structures with attenuation zones. Eng Struct 2013;56:1271–82.
[42] Huang J, Shi Z. Attenuation zones of periodic pile barriers and its application in vibration reduction for plane waves. J Sound Vib 2013;332:4423–39.
[43] Shi Z, Cheng Z, Xiang H. Periodic structures: theory and applications to seismic isolation and vibration reduction. Beijing, China: Science Press; 2017.
[44] Xiang H, Shi Z, Wang S, Mo Y. Periodic materials-based vibration attenuation in layered foundations: experimental validation. Smart Mater Struct 2012;21:112003.
[45] Huang HW. Periodic Metamaterials-based barriers for seismic isolation: field studies and computational modeling. University of Houston; 2020.
[46] Pu X, Meng Q, Shi Z. Experimental studies on surface-wave isolation by periodic wave barriers. Soil Dyn Earthquake Eng 2020;130:106000.
[47] Pu X, Shi Z. Broadband surface wave attenuation in periodic trench barriers. J Sound Vib 2020;468:115130.
[48] Huang HW, Zhang B, Wang J, Menq F-Y, Nakshatrala KB, Mo YL, et al. Experimental Study on Wave Isolation Performance of Periodic Barriers. Soil Dyn Earthquake Eng 2021;114.
[49] Huang HW, Wang J, Zhao C, Mo YL. Two-dimensional Finite Element Simulation of Periodic Barriers. ASCE J Eng Mech 2021;147:04020150.
[50] Brûlé S, Javelaud E, Enoch S, Guenneau S. Experiments on seismic metamaterials: molding surface waves. Phys Rev Lett 2014;112:133901.
[51] Zhang B, Huang HW, Menq F, Wang J, Nakshatrala KB, Stokoe KH, et al. Field experimental investigation on broadband vibration mitigation using metamaterial-based barrier-foundation system. Soil Dyn Earthquake Eng 2022;155:107167. https://doi.org/10.1016/j.soildyn.2022.107167.
[52] Menq F-Y, K. H. Stokoe I, Park K, Rosenblad BL, Cox BR. Performance of mobile hydraulic shakers at nees@UTexas for earthquake studies. 14th World Conference on Earthquake Engineering (WCEE). Beijing, China, 2008.